

On: 30 July 2014, At: 16:15

Publisher: Taylor & Francis

Informa Ltd Registered in England and Wales Registered Number: 1072954 Registered office: Mortimer House, 37-41 Mortimer Street, London W1T 3JH, UK



Journal of Sustainable Cement-Based Materials

Publication details, including instructions for authors and subscription information:

<http://www.tandfonline.com/loi/tscm20>

Numerical simulation of porosity on thermal properties and fire resistance of foamed concrete

Qiang Li ^a, Hao Wang ^a, Zuhua Zhang ^a & Andrew Reid ^b

^a Faculty of Engineering and Surveying, Centre of Excellence in Engineered Fibre Composites (CEEFC), University of Southern Queensland, Toowoomba, Australia

^b Haald Engineering Pty Ltd., Brisbane, Australia

Published online: 21 Jan 2013.

To cite this article: Qiang Li, Hao Wang, Zuhua Zhang & Andrew Reid (2013) Numerical simulation of porosity on thermal properties and fire resistance of foamed concrete, *Journal of Sustainable Cement-Based Materials*, 2:1, 13-19, DOI: [10.1080/21650373.2012.755748](https://doi.org/10.1080/21650373.2012.755748)

To link to this article: <http://dx.doi.org/10.1080/21650373.2012.755748>

PLEASE SCROLL DOWN FOR ARTICLE

Taylor & Francis makes every effort to ensure the accuracy of all the information (the "Content") contained in the publications on our platform. However, Taylor & Francis, our agents, and our licensors make no representations or warranties whatsoever as to the accuracy, completeness, or suitability for any purpose of the Content. Any opinions and views expressed in this publication are the opinions and views of the authors, and are not the views of or endorsed by Taylor & Francis. The accuracy of the Content should not be relied upon and should be independently verified with primary sources of information. Taylor and Francis shall not be liable for any losses, actions, claims, proceedings, demands, costs, expenses, damages, and other liabilities whatsoever or howsoever caused arising directly or indirectly in connection with, in relation to or arising out of the use of the Content.

This article may be used for research, teaching, and private study purposes. Any substantial or systematic reproduction, redistribution, reselling, loan, sub-licensing, systematic supply, or distribution in any form to anyone is expressly forbidden. Terms &

Conditions of access and use can be found at <http://www.tandfonline.com/page/terms-and-conditions>

Numerical simulation of porosity on thermal properties and fire resistance of foamed concrete

Qiang Li^{a*}, Hao Wang^a, Zuhua Zhang^a and Andrew Reid^b

^aFaculty of Engineering and Surveying, Centre of Excellence in Engineered Fibre Composites (CEEFC), University of Southern Queensland, Toowoomba, Australia; ^bHaald Engineering Pty Ltd., Brisbane, Australia

(Received 20 November 2012; Revised 10 December 2012; Accepted 12 December 2012)

The relationship between thermal insulation properties and porosity of fly ash based foam concrete was built, in which effective density, effective heat conductivity, and effective specific heat of fly ash based foam concrete were deduced as functions of porosity. Using the model, the effective heat conductivity of density of 580 kg/m³ fly ash based foam concrete was the theoretically calculated as 0.145 W/(m K) while the experimental measured value was 0.142 W/(m K). The relative error of heat conductivity was very low at 2.1%. The effective specific heat within the model was 967.05 J/kg K and the experimental value was 920 J/kg K with a relative error of 5.1%. Then, the effective heat conductivity and specific heat models were incorporated into heat transferring model to calculate the temperature field of fly ash based foam concrete wall during a fire incident. Finally, the temperature field of fly ash based foam concrete wall and traditional dense concrete wall during fire incident were calculated and compared. Comparing the temperature field of the fly ash based foam concrete wall with the traditional concrete wall, it was found that at close to fire-side surface, the temperature in the fly ash based foam concrete wall could reach 1039 °C, while the lowest temperature in the fly ash based foam concrete wall remained at 20 °C for a thickness of 7 mm. In contrast, at close to fire side of surface, the temperature of traditional concrete wall was 987.2 °C at 360 s and the lowest temperature in the traditional wall was 102.9 °C at the opposite side-wall surface far away from the fire direction. As expected, the data demonstrated that the use of fly ash based foam concrete in wall construction adds greatly to the time for people to leave in safety.

Keywords: foam concrete; porosity; effective heat conductivity; effective specific heat; temperature field

1. Introduction

As global warming becomes more evident, energy saving is an urgent priority around the globe, which requires more and more foamed construction materials for both residual and commercial buildings. The foamed concrete is lighter in weight for ease of transportation and of porous

structure for better thermal insulation. In the past decades, this field had aroused lots of research interest [1–5]. Several foamed concretes have been developed, including newspaper sandwiched aerated light weight concrete [5] and fly ash based light weight foamed concrete [6–11]. Using fly ash to produce foamed concrete

*Corresponding author. Email: Qiang.li@usq.edu.au

has an extra environmental benefit because of reutilization of waste material from power station [6,7,12].

Foamed, or aerated, structure will lose some of mechanical properties of the concrete [1–3]. A balanced combination of thermal insulation properties and mechanical properties is an important aspect in foamed concrete design. Different numerical models have been developed to calculate and optimize the foamed structure and its resulted properties. Costa et al. [8] adopted a numerical method to calculate the heat flux through the wet porous wall that considered the effects of liquid water and water vapor. Kunhanandan and Ramamurthy [9] presented a model for predicting the foam strength that considered the porosity. Bentz et al. [10] developed a relationship between thermal conductivity and density of fly ash concrete. Most of the published modeling work on porosity and properties were semi-experimental, which can only be used to the material system they used. In order to develop a universal model to describe the influence of porosity on thermal insulation, the first step is to calculate the effective density, the effective heat conductivity, and the effective specific heat of the foamed concrete. And then, these thermal properties were incorporated into a heat transfer model to calculate the temperature field of the foamed concrete. The results will be compared with traditional solid concrete to illustrate the effect of porosity on thermal insulation and fire resistance in a fire incident.

2. Physical model

To construct a representative model, the following assumptions are used:

- (1) The foamed concrete can be regarded as two phases, concrete being the matrix and air voids.

- (2) Each pore in the foamed concrete is regarded as an isolated pore that is not connected with others, and the pore is distributed uniformly in the whole simulated zone.
- (3) Heat conductivity, specific heat and density of concrete and air, and their interface heat transfer coefficient are all regarded as constants at all temperatures.

According to above assumptions, the density of the foamed concrete can be described as:

$$\rho = \rho_c(1 - \varepsilon) + \varepsilon\rho_a \quad (1)$$

where, ρ_c is concrete density. Fly ash based geopolymer concrete is used as the concrete matrix in this study, $\rho_c = 1373 \text{ kg/m}^3$. ρ_a is air density for the air void, and $\rho_a = 1.20 \text{ kg/m}^3$ [13]. ε is volume fraction of foam, and can be determined if the density (ρ) of the foamed concrete is measured. For example, if ρ is 580 kg/m^3 , $\varepsilon = (1373 - 580)/(1373 - 1.2) = 0.578$.

The effective heat conductivity can be expressed as:

$$\lambda = \lambda_c \frac{\lambda_c - (\lambda_c - \lambda_a)\varepsilon^2}{\lambda_c - (\lambda_c - \lambda_a)(\varepsilon^2 - \varepsilon)} \quad (2)$$

where, λ is the effective heat conductivity of foamed concrete. Air heat conductivity, λ_a , is 0.024 W/(m K) [13]. Heat conductivity of the concrete matrix, λ_c , is 0.369 W/(m K) . If taking $\varepsilon = 0.578$ into Equation (2), the effective heat conductivity will be 0.145 W/(m K) . The actual measured value from the 580 kg/m^3 sample is 0.142 W/(m K) , which indicates that the heat conductivity model well predicts the experimental value (relative error 2.1%).

According to Ref. [10], the effective specific heat of the foamed concrete can be written as:

$$C_p = C_p^a m_a + C_p^c (1 - m_a) \quad (3)$$

where, m_a is the mass fraction of the foam, which can be calculated from $m_a = \rho_a \times \varepsilon / [\rho_a \times \varepsilon + \rho_c \times (1 - \varepsilon)]$. For 580 kg/m^3 foamed concrete, $m_a = 0.0012$. C_p^a is the specific heat of air, which is 1005 J/kg K [13]. C_p^c is specific heat of the concrete matrix, which is 967 J/kg K . So, the effective specific heat of the foamed concrete can be calculated: $C_p = 967.05 \text{ J/kg K}$. Compared with the actual measured value 920 J/kg K , the relative error is only 5.1%.

The heat transfer in foamed concrete wall can be expressed as:

$$\frac{\partial T}{\partial t} = \alpha \nabla^2(T) \quad (4)$$

where, T is temperature ($^{\circ}\text{C}$); t is time (s); and α is thermal diffusivity (m^2/s), which can be expressed as $\alpha = \frac{\lambda}{\rho C_p}$, where λ is thermal conductivity from Equation (2), ρ is effective density from Equation (1), and C_p from Equation (4).

When there is a fire outside the wall, temperature rising curve of fire incident can be given as a function of firing time [14]:

$$T_f = 20 + 345 \ln(1 + 8t) \quad (5)$$

At the beginning of fire incident, the initial temperature of the wall (both

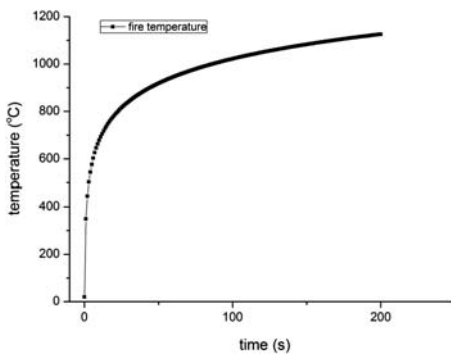


Figure 1. Fire temperature curve.

inside and outside) is set $T_o = 20^{\circ}\text{C}$. Fire temperature rising curve can be seen in Figure 1.

In the outside of the wall, the convection and radiation heat transfer will be applied:

$$\frac{\partial T}{\partial t} = -h_o(T_3 - T_f) \quad (6)$$

where, h_o is the interface heat transfer coefficient between the fire surrounding and the outside wall surface; T_3 and T_f are fire surrounding temperature and outside wall surface temperature, respectively.

In the inside of the wall, the same convection and radiation heat transfer equation is applied:

$$\begin{aligned} \frac{\partial T}{\partial t} &= -h_i(T_2 - T_1) \\ q &= \epsilon_1 \sigma A_1 (T_1^4 - T_2^4) \end{aligned} \quad (7)$$

where, h_i is the interface heat transfer coefficient between the inside wall surface and inside room surrounding; T_2 and T_1 are the inside room surrounding temperature (20°C) and inside wall surface temperature, respectively; ϵ_1 is grey body emissive coefficient, in this paper, its value is adopted as 0.63 [13]; σ is Stefan–Boltzmann constant, which is $5.669 \times 10^{-8} \text{ W/m}^2 \text{ K}$; and A_1 is the area of emissive zone (m^2).

In order to reduce the calculating time, a 30 mm thickness wall is adopted and the wall section is with a length and width of 10 mm, and the length and width direction are set as periodic boundary conditions. This means that there is no heat transfer happening except inside and outside of the wall. The temperature field for a solid concrete wall under the same condition and same size is also modeled for comparison. The density, heat conductivity, and specific heat of the solid concrete are 2300 kg/m^3 , 1.8 W/m K , and 912 J/kg K , respectively. The

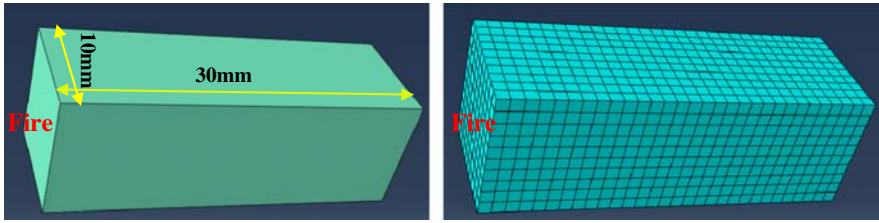


Figure 2. A schematic figure of wall and its meshed figure.

meshed size is 1 mm, and the wall is meshed into 3000 cubic units. The schematic figure and meshed shape can be seen in Figure 2.

3. Results and discussion

Figure 3 shows the temperature field in the foamed concrete wall at different time,

0.03, 99, 200, and 360 s. The colors in each figure stand for the different temperature values. At 0.03 s, in Figure 3(a), only the very end of the fire side wall has temperature rise from initial 20 to 22 °C. When the time is 100 s, in Figure 3(b), the temperature of the outside wall surface rises quickly to 1045 °C, and temperature-raised zone has been extended to the 11th

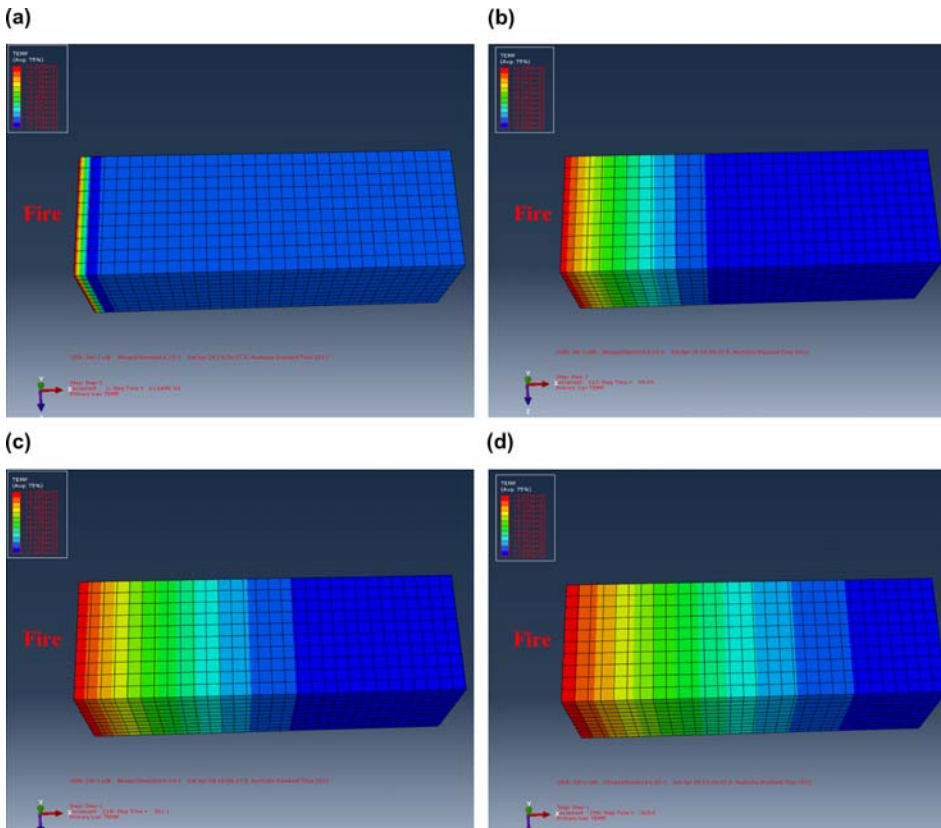


Figure 3. Temperature field of foamed concrete at different time: (a) 0.03 s; (b) 100 s; (c) 200 s and (d) 360 s.

meshed grid. In another word, there is still 19 mm in depth of the wall kept its temperature unchanged at 20 °C at 100 s. At 200 s, when the fire stops, (Figure 3(c)) the maximum temperature is 1058 °C, and the unchanged temperature zone is 13 mm in depth of wall. In Figure 3(d), the highest temperature drops to 1039 °C at 360 s and there are still 7 mm in depth of wall unchanged its initial temperature 20 °C.

Figure 4 shows temperature rising curve in the 10 selected units of the

foamed concrete. From the left side of wall, the temperature evolution curve of the first unit can be seen in the top two lines, which indicates that the temperature rise quickly from 0 to 50 s, and then, the temperature rising is slow down. The final temperature difference between the two lines is about no more than 50 °C. As the unit is 1 mm in size, therefore, the temperature gradient is about 50 °C/mm at 360 s for the first unit. In the units away from the external fire, the temperature gap

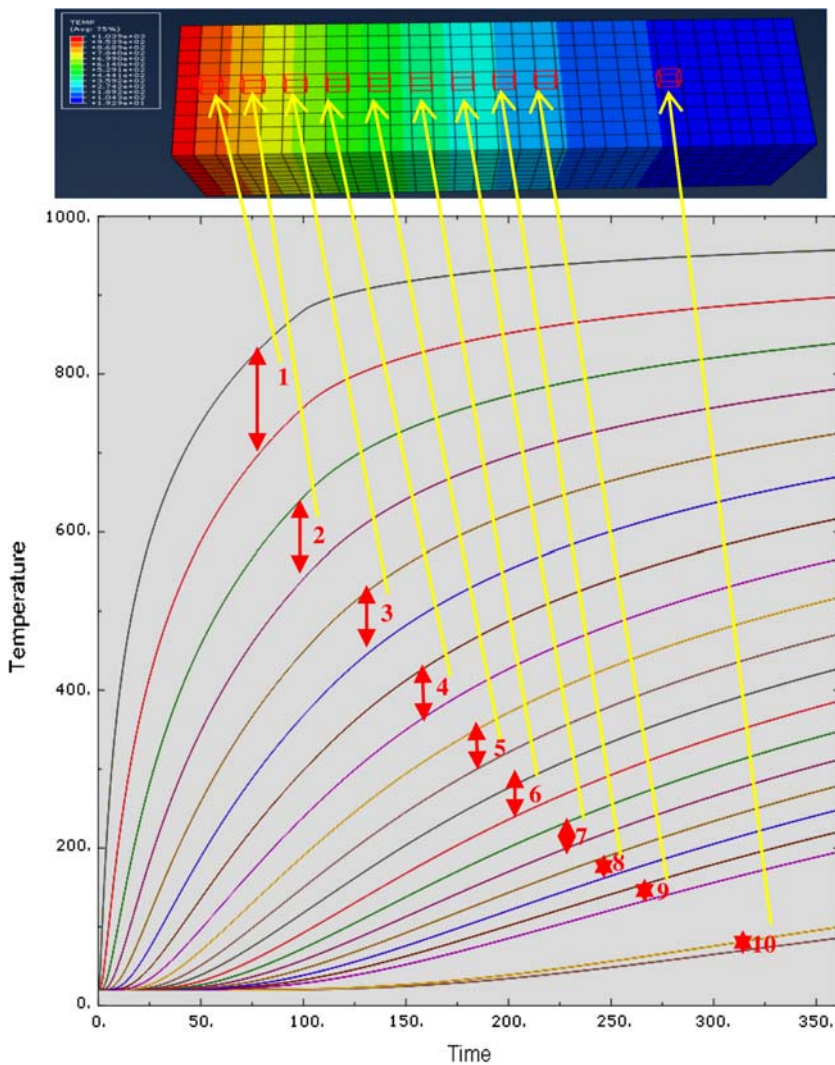


Figure 4. Temperature evolution curve of the selected unit during fire incident.

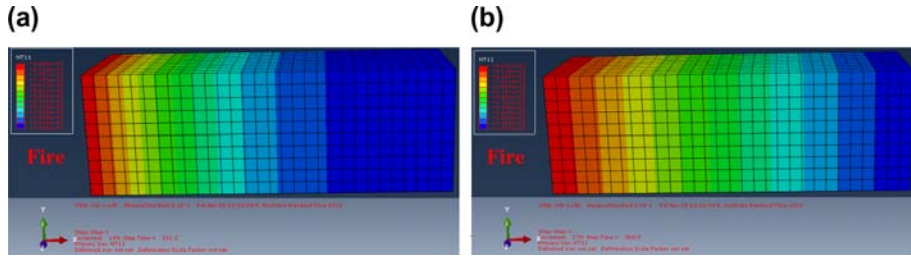


Figure 5. Temperature field of solid concrete wall at different time: (a) 100 s and (b) 360 s.

decreases gradually. For the last selected unit, the temperature difference between the two sides of the unit is 20°C at 360 s.

Figure 5 shows temperature field of traditional concrete wall at different times, 100 and 360 s. At 100 s (Figure 5 (a)), the highest temperature and the lowest temperature are 948 and 30°C , respectively, and located in wall surface of the fire side wall and far end of the other side. At 360 s (Figure 5(b)), the highest and lowest temperatures are 987 and 102°C , respectively, which mean that

there are no places being under 100°C . Compared with foamed concrete at the same time (Figure 3(d)), the solid concrete has much fast temperature rise.

Figure 6 shows the temperature evolution curve of different positions in the solid concrete. Six nodes are chosen along the wall thickness. The first node is closest to the fire, and its temperature rises quickly to 700°C at the beginning, the first 50 s, then, gradually rises to 800°C at 100 s. The temperature rise becomes very slow afterward. It is 900°C at 360 s. The

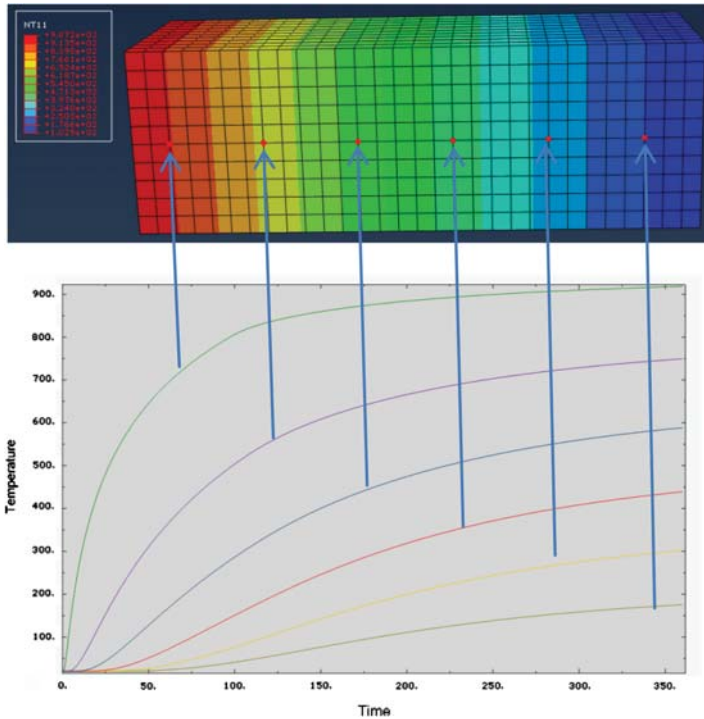


Figure 6. Temperature evolution curve of the marked point.

second node next to it has a slower temperature rising. At 360 s, it reaches 700 °C. In the last node, which is located at 3 mm away from the inside wall surface, the temperature rise is very slow, but it still reaches 180 °C at 360 s.

4. Conclusions

Relatively simple finite element models are employed to demonstrate the superior fire resistance of foamed concrete over solid concrete. Effective heat conductivity model and effective specific heat model are built to calculate thermal diffusivity, which is used in the final heat transfer model. Temperature fields of foamed concrete and solid concrete during a fire incident are calculated using the heat transfer model. For a 30 mm thickness wall, the foamed concrete still has 7 mm thick of the inside wall at 20 °C in 360 s after fire. While the solid concrete evens the inside wall, surface has the temperature raised to 150 °C.

References

- [1] Schenker A, Anteby I, Nizri E, Ostraich B, Kivity Y, Sadot O, Haham O, Mechelis R, Gal E, Ben Dor G. Foam-protected reinforced and concrete structure under impact: experimental and numerical studies. *J. Struct. Eng.-ASCE* 2005;131:1233–1242.
- [2] Lian C, Zhuge Y, Beecham S. The relationship between porosity and strength for porous concrete. *Constr. Build. Mater.* 2011;25:4294–4298.
- [3] Benazzouk A, Douzane O, Mezreb K, Laidoudi B, Queneudec M. Thermal conductivity of cement composites containing rubber waste particles: experimental study and modelling. *Constr. Build. Mater.* 2008;22:573–579.
- [4] Matusinovic T, Sipusic J, Vrbos N. Porosity–strength relation in calcium aluminates cement pastes. *Cem. Concr. Res.* 2003;33:1801–1806.
- [5] Soon-Ching NG, Kaw-Sai Low. Thermal conductivity of newspaper sandwiched aerated lightweight concrete panel. *Energ. Build.* 2010;42:2452–2546.
- [6] Kearsley EP, Wainwright PJ. Ash content for optimum strength of foamed concrete. *Cem. Concr. Res.* 2002;32:241–246.
- [7] Kunhanandan Nambiar EK, Ramamurthy K. Influence of filler type on the properties of foam concrete. *Cem. Concr. Comp.* 2006;28:475–480.
- [8] Costa VAF, Mendonc ML, Figueiredo AR. Modelling and simulation of wetted porous thermal barriers operating under high temperature or high heat flux. *Int. J. Heat Mass Tran.* 2008;51:3342–3354.
- [9] Kunhanandan Nambiar EK, Ramamurthy K. Models for strength prediction of foam concrete. *Mater. Struct.* 2008;41:247–254.
- [10] Bentz DP, Peltz MA, Dura'n-Herrera A, Valdez P, Jua'rez CA. Thermal properties of high-volume fly ash mortars and concretes. *J. Build. Phys.* 2011;34:263–275.
- [11] Sumanasooriya Milani S, Neithalath Narayanan. Pore structure features of pervious concretes proportioned for desired porosities and their performance prediction. *Cem. Concr. Comp.* 2011;33:778–787.
- [12] Ahmaruzzaman M. A review on the utilization of fly ash. *Prog. Energ. Combust.* 2010;36:327–363.
- [13] Holman JP. *Heat transfer*, 9th ed. Beijing: China Machine Press; 2005.
- [14] Yushu Wang, Chuanguo Fu. *Abaqus structural engineering analysis and examples to explain*. Beijing: Chinese constructional industrial Press; 2011.